

Optical Leaky Waveguide Sensor for Detection of Bacteria with Ultrasound Attractor Force

Mohammed Zourob,^{*,†,‡} Jeremy J. Hawkes,[†] W. Terence Coakley,[§] Bernard J. Treves Brown,[†] Peter R. Fielden,[†] Martin B. McDonnell,^{||} and Nicholas J. Goddard[†]

School of Chemical Engineering and Analytical Science, The University of Manchester, P.O. Box 88, Sackville Street, Manchester M60 1QD, U.K., Cardiff School of Biosciences, Cardiff University, Cardiff, Wales, CF10 3TL, U.K., and Dstl, Porton Down, Salisbury, Wiltshire SP4 0JQ, U.K.

An integrated, sensitive, and rapid system was developed for the detection of bacteria. The system combined an optical metal-clad leaky waveguide (MCLW) sensor with ultrasound standing waves (USW). The performance of a MCLW sensor for the detection of bacteria has been increased (>100 fold) by using USWs to drive bacteria onto the sensor surface. By forming the USW nodes at or within the surface of the MCLW, the diffusion-limited capture rate has been replaced by fast movement. Immobilized anti-BG antibody on the MCLW sensor surface was used to capture *Bacillus subtilis* var. *niger* (BG) bacterial spores driven to the surface. This combination of sensor and attractor force combination has been tested by detecting the evanescent scattering from bacterial spores at the sensor surface. Application of ultrasound for 3 min gave a detection limit for BG bacterial spores of 1×10^3 spores/mL.

The detection and characterization of bacteria without the need for a culture step is an important goal for microbiology. Rapid variant-specific sensing will facilitate new approaches to medical diagnosis, protection against bioterrorism, and food processing. Systems that can be miniaturized and automated offer a significant advantage over current technology, especially if detection is needed in the field.

Evanescent optical waveguide biosensors have the potential to obviate the need for culturing; Zourob et al.^{1,2} have used a metal-clad leaky waveguide (MCLW) to extend the evanescent fields $\sim 1 \mu\text{m}$ from the surface. This allows the relatively large bacterial spores of interest here to be detected by capturing them on an appropriate immobilized antibody on the MCLW sensor surface. Such sensors are very sensitive; with a 20-min exposure time they can detect concentrations of *Bacillus subtilis* var. *niger* (BG) spores

as low as 10^4 mL^{-1} .² This lengthy time period is due to the low diffusion coefficients for large analytes.

The use of ultrasound to move particles within a fluid is well known,³ the force (F) acting on the particles is described by

$$F_{\text{us}} = \left(\frac{P_0^2 V_p \beta_p \pi}{2\lambda} \right) \left(\frac{(5\rho_p - 2\rho_f)}{(2\rho_p + \rho_f)} - \frac{\beta_p}{\beta_f} \right) \sin\left(\frac{4\pi z}{\lambda}\right) \quad (1)$$

where P_0 is the peak sound pressure and ρ_p and ρ_f are respectively the particle and medium densities. β_p and β_f are the compressibilities of the particle and medium, respectively. λ is the wavelength of sound in the suspending phase. V_p is the particle volume, and z is the distance normal to the pressure node.

Hawkes et al.⁴ described an approach that meets the detector speed requirement by using radiation force of ultrasound standing waves rather than waiting for diffusion to drive BG bacterial spores onto immobilized anti-BG antibodies. The important feature of this approach is the movement of particles to a wall, in this case the MCLW, by placement of an ultrasound pressure node at the surface through the use of a half-wavelength reflector. At this specific thickness, some ultrasound is transmitted through the glass reflector, enabling a pressure node to form at the liquid/solid interface. An approximate calculation of the reflector thickness for transmission is obtained from sound transmission (T) through a plate between two infinite media indicates a maximum at half-wavelength thickness.

$$T = \frac{4}{2 + (Z_3/Z_1 + Z_1/Z_3) \cos^2 k_2 L + (Z_2^2/Z_1 Z_3 + Z_1 Z_3/Z_2^2) \sin^2 k_2 L} \quad (2)$$

where Z_1 , Z_2 , and Z_3 are the acoustic impedances of the first medium the plate and the final medium, respectively. k is the wavenumber, and L is the thickness of the plate⁵

In our system, where the fluid is only a quarter wavelength, a matrix approach is more appropriate and provides some quantita-

* To whom correspondence should be addressed. Tel: (+44) 161-3068884. Fax: (+44) 161-3064911. E-mail: m.zourob@manchester.ac.uk.

[†] The University of Manchester.

[‡] Present address: School of Materials Science, The University of Manchester, P.O. Box 88, Grosvenor St., Manchester M1 7 HS, U.K.

[§] Cardiff University.

^{||} Dstl.

(1) Zourob, M.; Mohr, S.; Treves Brown, B. J.; Fielden, P. R.; McDonnell, M. B.; Goddard, N. J. *Sens. Actuators, B* 2003, 90, 296–307.

(2) Zourob, M.; Mohr, S.; Treves Brown, B. J.; Fielden, P. R.; McDonnell, M. B.; Goddard, N. J. *Anal. Chem.* 2005, 77, 232–242.

(3) Chladni, E. E. F. *Die Akustik*; Brietkopt and Hartel: Leipzig, 1802.

(4) Hawkes, J. J.; Long, M. J.; Coakley, W. T.; McDonnell, M. B. *Biosens. Bioelectron.* 2004, 19, 1021–1028.

(5) Kinsler, L. E.; Frey, A. R.; Coppens, A. B.; Saunders, J. V. *Fundamentals of Acoustics*, 4th ed.; John Wiley and Son Inc.: New York, p 153.

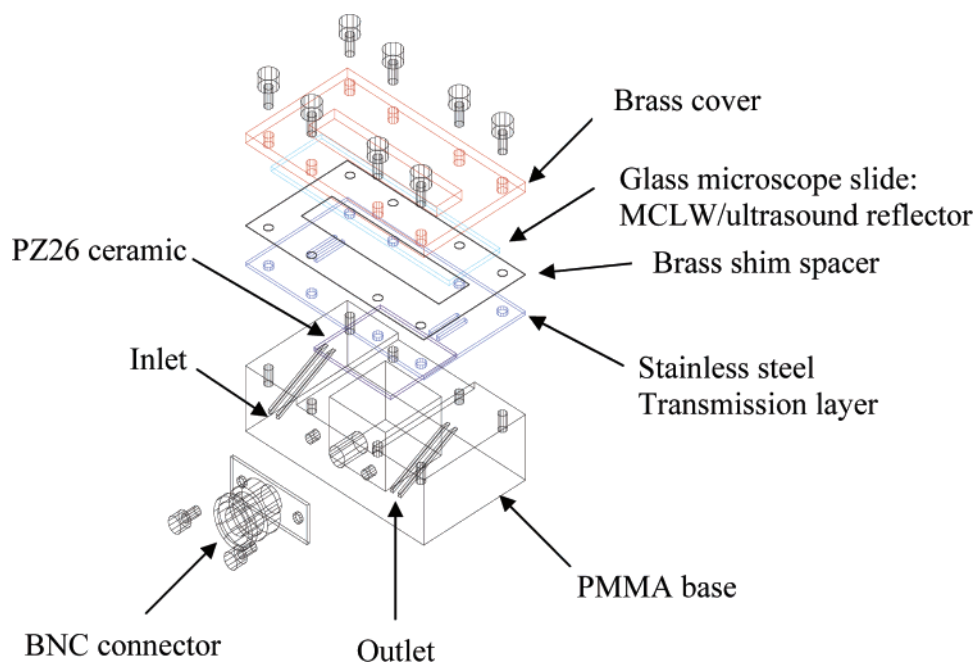


Figure 1. Ultrasound chamber construction.

tive pressure estimates.^{6,7} The chamber is only a quarter-wavelength long, and therefore, only one node forms to attract all the cells in the chamber. However, measurement of cell numbers was labor intensive, requiring the chamber to be disassembled to remove the antibody-coated reflector from the chamber for microscopic analysis. In this paper, the detection process is automated (measurements are made in the assembled chamber) by combining the metal-clad leaky waveguide and the ultrasound standing waves in one system.

EXPERIMENTAL SECTION

Materials and Methods. Normal microscope glass slides (Dow Corning) of 1-mm thickness were purchased from BDH (Poole, U.K.). (3-Aminopropyl)triethoxysilane (APTS), a suspension of 1.1 μm diameter latex beads, 25% glutaraldehyde (diluted to 5% before use), 10 mM phosphate buffer (PBS, pH 7.5), ethanolamine hydrochloride, bovine serum albumin (BSA), and HEPES-buffered saline, were purchased from Sigma (Gillingham, U.K.). BG spores were provided by Dstl (Porton Down, U.K.). Immediately before use, these were washed three times to remove competing antigen protein, centrifuged at 10000 rpm for 5 min, and resuspended in 10 mM HEPES-buffered saline. A dilution series of BG spore concentrations from 1×10^2 to $1 \times 10^{10} \text{ mL}^{-1}$ was made in HEPES buffer. Polyclonal rabbit anti-BG antibody solution was obtained from Dstl, at a concentration of 5.7 mg mL^{-1} . This stock was diluted with PBS to obtain an antibody concentration of 100 $\mu\text{g mL}^{-1}$.

Metal-Clad Leaky Waveguide/Ultrasound Reflectors. The 1-mm glass slides have been shown⁴ to be half-wavelength ultrasound reflectors, as required to form a node in the region of the reflector, at frequencies of $\sim 3 \text{ MHz}$. The waveguiding layers of the MCLW were coated by IMEC (Louvain, Belgium). The

1-mm glass slides were coated with 8.5 nm of titanium followed by a 300-nm-thick layer of silica.

Antibody Immobilization. MCLW-coated glass slides were cleaned by rinsing with deionized water and then dried at room temperature. Next the slides were soaked in 10% APTS for 1 h and then thoroughly washed with deionized water. The surface was then activated with 5% glutaraldehyde for 2 h and again thoroughly rinsed using deionized water. The MCLW chip surface were exposed to anti-BG antibodies at 100 $\mu\text{g mL}^{-1}$ in 10 mM phosphate buffer (pH 7.5) for 2 h. The 1 M ethanolamine hydrochloride (pH 8.5) was then used to block the remaining active surface sites. Finally, 5% BSA was run through the flow cell over the slides to reduce nonspecific binding.²

Ultrasound Chamber Construction and Control System. The basic construction of the flow chamber (Figure 1) was as described by Hawkes et al.⁴ In this work, the glass microscope slide used as a half-wavelength acoustic reflector was coated, as described above, to form an antibody-coated MCLW. The flow channel was defined by a 0.125-mm brass spacing element with a slot of $60 \times 10 \text{ mm}$. The ultrasound field was produced in a $10 \times 20 \text{ mm}$ region at the center of this channel. BG spore suspension was pumped into the chamber through 1.2-mm-i.d. tubing connected to the inlet and outlet ports at 200 $\mu\text{L min}^{-1}$ using a peristaltic pump (Minipuls-3, MP4, Gilson Inc.).

Generation and control of the frequency and voltage applied to the transducer were achieved as described elsewhere.^{8,9} This provided sinusoidal power across a range of frequencies and allowed measurement of voltage at the ultrasound transducer.

Optical Waveguide/Ultrasound Standing Waves Setup. A schematic of the positioning of the chamber with respect to the laser and camera is shown in Figure 2. The laser was mounted on conventional optical posts and carriers (Melles Griot, Irvine,

(6) Hawkes, J. J.; Gröschl, M.; Benes, E.; Nowotny, H.; Coakley, W. T. *Rev. Acoust.* **2002**, 33, PHA-01-007-IP.

(7) Nowotny, H.; Benes, E. *J. Acoust. Soc. Am.* **2002**, 82, 513–521.

(8) Spengler, J. F.; Jekel, M.; Christensen, K. T.; Adrian, R. J.; Hawkes, J. J.; Coakley, W. T. *Bioseparation* **2001**, 9, 329–341.

(9) Hawkes, J. J.; Coakley, W. T. *Enzyme Microb. Technol.* **1996**, 19, 57–62.

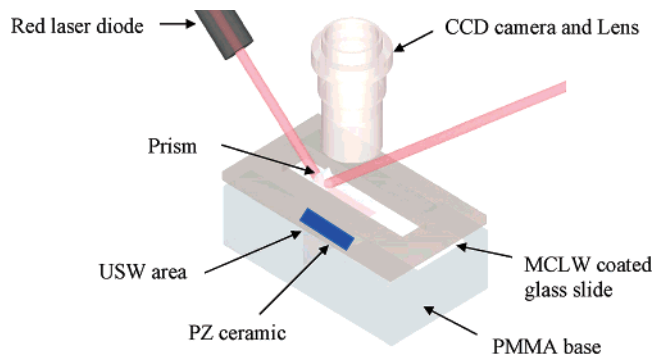


Figure 2. Schematic of the ultrasound-MCLW instrumental setup.

CA), installed on an optical rail (Melles Griot). The rail mounting allowed it to rotate in the vertical plane with the axis of rotation passing through the flow chamber/prism assembly. Rotation of the rail allowed adjustment of the laser beam input angle relative to the prism. At a laser angle of $\sim 28^\circ$ with respect to the MCLW chip, the TE_0 evanescent field illuminates the particles in contact with the MCLW surface while the other areas of the chamber remaining dark.

A 6-mm equilateral prism (BK7 glass), refractive index 1.510, was coupled with 1.517 refractive index matching oil (Cargille Labs, Cedar Grove, NJ) to the outside of the MCLW microscope slide in the chamber in an area close to, but not within, the sound irradiation zone (see Figure 2). This allowed light incident on the prism at $\sim 28^\circ$ to pass freely through the microscope slide into the waveguide substrate inside the chamber.

For production of scattered light, a 3-mW semiconductor laser (RS Components Ltd., $\lambda_{\text{max}} = 635 \text{ nm}$) was used. The laser light coupled through the BK7 prism into the waveguide structure. A digital camera (Pulnix TM-1001, Pulnix America Inc., Sunnyvale, CA) was used to observe the scattering. The camera consists of a high-resolution 1-in. monochrome progressive scanning 1024 (H) \times 1024 (V) interline transfer CCD imager; it was fitted with a DIN achromatic microscope objective (10 \times , 0.25 NA), with a 180 μm field of view (Edmund Optics Ltd., Clifton Moor, York, U.K.). The images were collected using a framegrabber card (Data Translation (Marlboro, MA) mounted in a standard personal computer. Quantification of the signal intensity from the light scattering for a particular particle was calculated by summing all the pixels belonging to that particle whose value exceeded a preset threshold value. The monitoring and image analysis were controlled by software written in-house using the LabVIEW programming environment (National Instruments, Austin, TX). The figure was generated after feeding the captured image from the camera to MATLAB (v 6, Math Work, Inc., Natick, MA) to convert the image from a 2-D matrix into a 1-D histogram (x, y). Hence, x represents the pixel intensity and y represents the frequency (number of particles having the same intensity).

RESULTS AND DISCUSSION

Operating Frequencies. The operating frequency of the chamber used in cell manipulation was found by comparing voltage: frequency spectra measured across the transducer with the chamber first air-filled and then water-filled. The ultrasound frequency was stepped through 100 equal increments between 2 and 4 MHz with a constant 0.05 $V_{\text{p-p}}$ applied to the amplifier. The

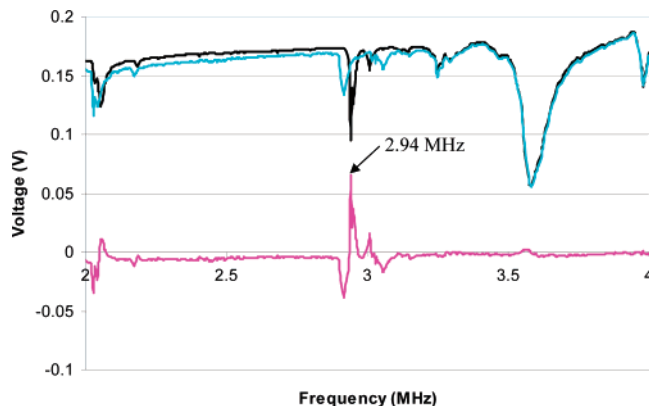


Figure 3. Frequency spectrum for the ultrasound chamber, empty (black line), filled with water (light blue line), and the difference between the two (magenta line). The frequency for operation is identified as 2.94 MHz.

frequency of maximum difference between these two spectra was assumed to be due to the resonance in the water and therefore chosen as the approximate operating frequency. The measured spectra are shown in Figure 3. The frequency (2.94 MHz) of the maximum voltage difference between the empty and water-filled chamber was chosen as the operating frequency. This operating frequency resulting in 0.44 $V_{\text{p-p}}$ at the transducer was when 0.05 $V_{\text{p-p}}$ was applied to the amplifier.

Small manufacturing variations in the microscope slides has been shown to produce slight changes to the resonant frequency of the system.¹⁰ Therefore, before each reflector was used, with BG spores tests were carried out with 1.1- μm -diameter latex bead suspensions to operationally confirm the exact drive frequency at which the suspended particles would make contact with the ultrasound reflector/MCLW. These did not adhere to the anti-BG and were then washed away before tests with BG spores.

Light Scattering Produced by BG Spores. For each experimental run with BG bacterial spores, the flow rate was set to 200 $\mu\text{L min}^{-1}$. In the absence of ultrasound, a suspension of BG bacterial spores ($10^7 \text{ spores/mL}^{-1}$) flowing through the chamber produced a small number of discrete points of scattered light randomly distributed across the cameras field of view. Image processing was used to convert this to the particle count shown in Figure 4a. Video observations also showed that individual spores were carried by the flow along the surface of the reflector, before suddenly stopping and adhering in the manner described by Perkins and Squirrell¹¹ and attributed by them to spore interaction with the antibody.

The sound was applied for a 3-min time interval immediately while the BG spore suspension solution flowed through the chamber. When the ultrasound (0.5 V) was turned on, a small number of spore "clumps" formed in the central region of the chamber and were held stationary against the flow. The size of the clumps increased with exposure time as more spores flowed into the system, as shown in Figure 4b. When the ultrasound was turned off and the flow cell was washed with buffer (at 200 $\mu\text{L min}^{-1}$), the remaining spores on the sensor surface indicated that these spores are captured by the antibody (Figure 4c).

(10) Martin, S. P.; Townsend, R. J.; Kuznetsova, L. A.; Borthwick, K. A. J.; Hill, M.; McDonnell, M. B.; Coakley, W. T. *Biosens. Bioelectron.* In press.

(11) Perkins, E. A.; Squirrell, D. J. *Biosens. Bioelectron.* **2000**, *14*, 853–859.

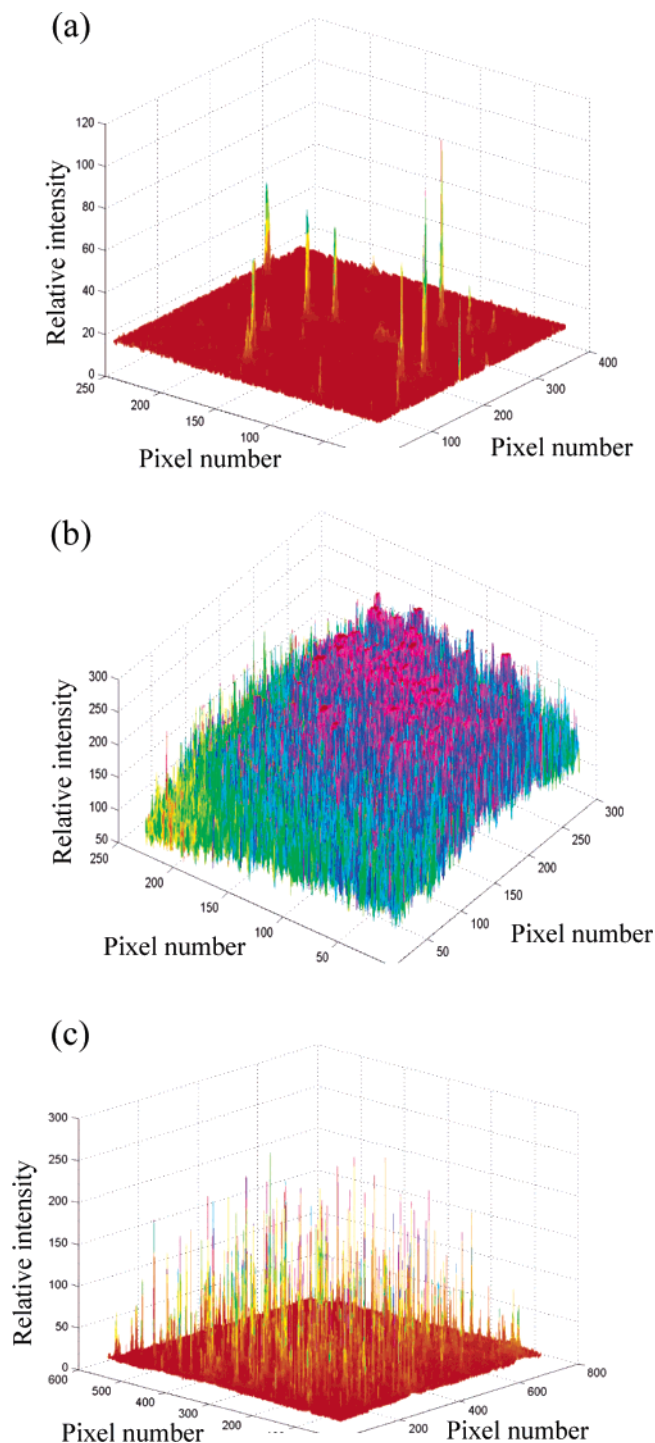


Figure 4. Detection of BG bacteria spores in a 1×10^7 spores/mL suspension (a) before (b) during the application of $4.5 V_{p-p}$ at the ultrasound transducer (c) captured BG after ultrasound application.

A solution of 1×10^6 spores/mL was pumped through the ultrasound-MCLW system to determine the pushing efficiency of bacteria onto the MCLW surface. It was assumed that a typical BG bacterium spore is a sphere of $1\text{-}\mu\text{m}$ diameter; therefore, the flow cell area can accommodate a maximum of 1×10^6 spores/ mm^2 as a monolayer onto the MCLW surface. It was found that the ultrasound pushed over 96% of BG bacteria spores from the bulk solution onto the MCLW sensor surface. This ratio is calculated by dividing the number of particles that filled the

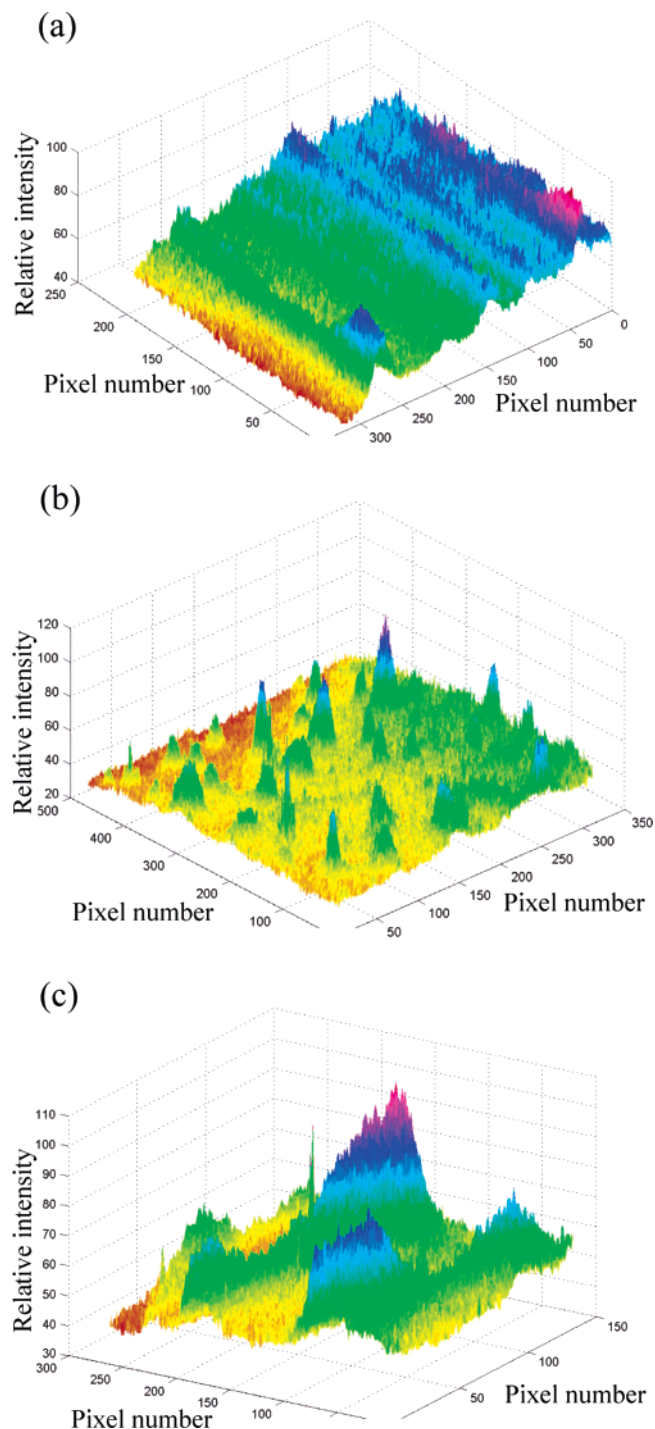


Figure 5. Illustration of the different patterns of 1×10^7 BG spores/mL suspension that can be obtained using ultrasound (a) strips (obtained at 3.35 MHz), (b) small clumps (obtained at 3.15 MHz), and (c) wavelike lines (obtained at 3.52 MHz).

chamber and the number of particles pushed on the MCLW surface.

Patterning. When the ultrasound was turned on, the BG bacteria spores did not form a uniform mat across the reflector face but produced a regular patterns, such as small clumps, strips, and wavelike lines. A change in drive frequency of 150 kHz was sufficient to move from one pattern type to another. Some of the patterns obtained are shown in Figure 5. They resemble the vibration modes described by Ernst E. F. Chladni in *Die Akustik*

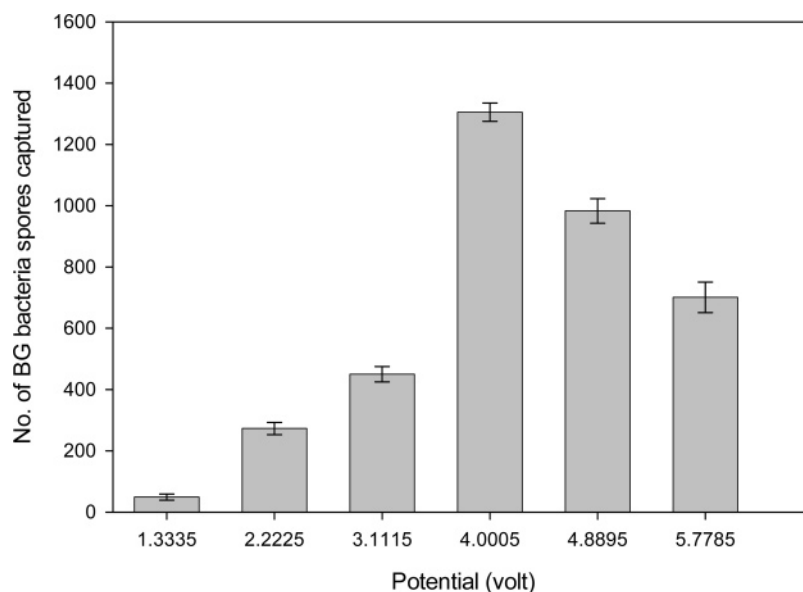


Figure 6. Effect of applied voltage on the number of BG bacteria spores deposited onto the MCLW over a time interval of 3 min. Error bars represent ± 1 standard deviation, $n = 5$.

1802,³ updated by Rossing.¹² Similar localized concentrations of particles in suspension have also been observed in a half-wavelength system.¹³ This effect makes formation of entirely uniform coatings difficult, but control of the patterns could lead to deposition of particles in preferred regions of the surface.

Influence of Applied Voltage on Spore Capture. Figure 6 shows the relationship between voltage (voltage is proportional to sound pressure) and the number of BG bacterial spores deposited onto the MCLW surface over a time interval of 3 min. A rapid increase in spore attraction is observed up to $4 V_{p-p}$; this is in agreement with the expectation of a squared relationship between pressure and force on the particle.¹⁴ Above $4 V_{p-p}$, spore aggregates were observed; these would limit contact of BG with the immobilized antibody and could account for the fall in captured spores beyond $4 V_{p-p}$.

Deposition Areas. The difference in deposition in relation to specific regions of the MCLW can be seen in Figure 7. Little or no deposition occurred before the spores reached the ultrasound field (position a in Figure 7), where as maximum deposition occurred within the field (position b in Figure 7). A small number of BG bacterial spores were deposited in the region beyond the field, after the flow had carried the spores past the area in front of the electrode covered by the piezoceramic (position c in Figure 7). Spore binding approaches saturation at the region of maximum attachment (position b in Figure 7). The reduced amount of attachment further downstream (position c in Figure 7) may be accounted for by the reduced concentration of spores near the surface due to earlier spore removal from suspension.

Influence of Spore Concentration. The general position of the spore clumps in the chamber did not change during a frequency scan from 2.930 to 2.950 MHz. This enabled the effect of changing the spore concentration to be examined, while ensuring that the same areas of the chamber could be compared to each other. The regions of maximum spore adherence, at the

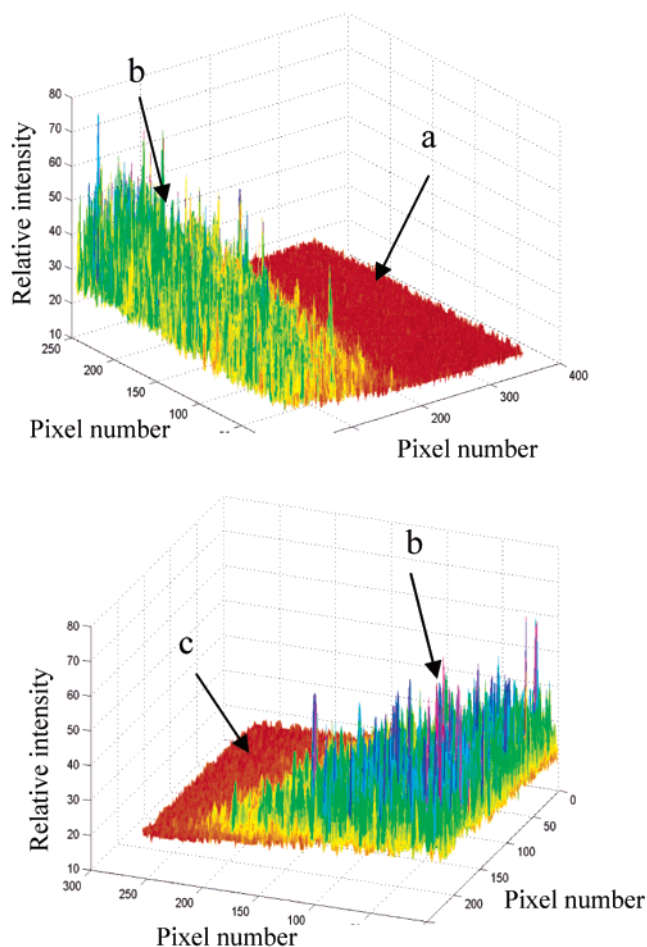


Figure 7. Deposition of BG spores from suspension (10^6 mL^{-1}) flowing through the chamber before (a), within (b), and after (c) the ultrasound electrode area.

(12) Rossing, T. D. *Am. J. Phys.* **1982**, *50*, 271–274.

(13) Spengler, J. F. Ph.D. Thesis, Technical University of Berlin, Germany, 2002.

(14) Gröschl, M. *Acustica* **1998**, *84*, 815–822.

center of the clumping patterns, were compared using different concentrations of bacteria spores.

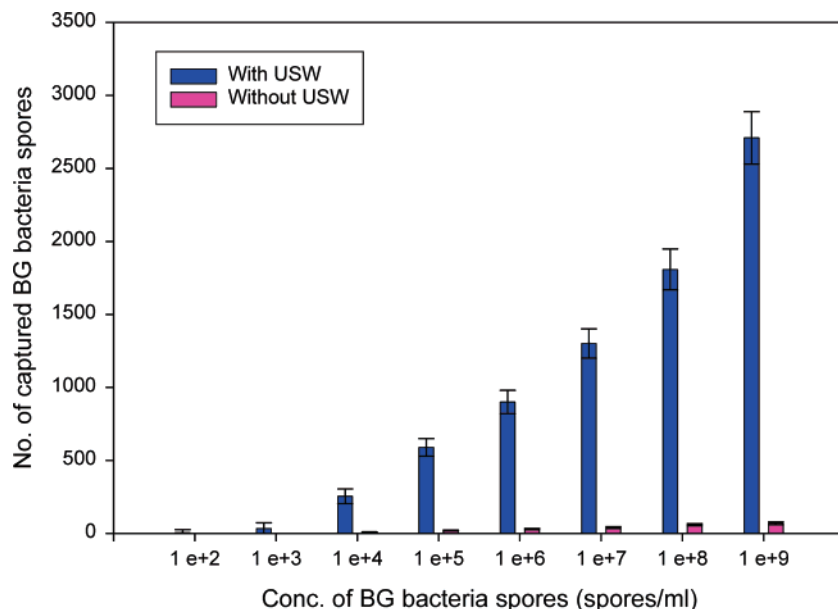


Figure 8. Relationship between the number of BG spores deposited and concentration of BG spore suspensions. Error bars represent ± 1 standard deviation, $n = 4$.

Figure 8 compares the number of BG bacterial spores captured at the MCLW chip surface at spore concentrations in the suspension over a range of 1×10^2 – 1×10^9 spores/mL on to the sensor surface with and without using the USW. This was achieved by counting the number of BG bacterial spores deposited from the images taken over the area of the evanescent field propagation, for 3 min. The limit of detection was found to be 1×10^3 cells/mL when the USW was applied for 3 min. This value has been taken as the concentration that gave a signal three times the background noise. It is clear from Figure 8 that the ultrasound enhances the deposition of BG to the immobilized anti-BG, which resulted in a shortened analysis time.

The radiation force that pushes cells to a pressure node is proportional to the particle (or acoustical inhomogeneity) volume (eq 1), as is the much weaker radiation force that moves cells within the nodal plane.¹⁵ Cell aggregates therefore can be manipulated more easily than single particles. The marked increase in spore attachment with increasing spore concentration, shown in Figure 8, might also suggest that spore aggregation, induced by interparticle acoustic forces,⁷ is creating spore clusters in suspension. It is clear, however, from Figure 4c that a large number of bacteria spores were attached to the MCLW sensor surface as individual particles.

CONCLUSION

It has been shown that combining the USW and MCLW improved the detection limit and shortened the time of analysis. The results show that it has been feasible to develop an integrated, rapid, and sensitive biosensor for bacterial detection. Ultrasound standing waves significantly enhance the capture of BG spores from a flowing sample onto an immunocoated optical leaky waveguide surface by providing an attraction force that moves them directly across the lines of flow. For this proof-of-principle work, we have combined two known techniques without significant adaptation, both of these are at an early stage in their development and the procedures are likely to be simplified and become more efficient. The use of a polymer reflector would, for example, enhance the ultrasound force and the MCLW efficiency.

ACKNOWLEDGMENT

The authors gratefully acknowledge financial support for M.Z. from the U.K. Government and The University of Manchester through an Overseas Research Studentship (ORS). They also gratefully acknowledge funding from the U.K. Ministry of Defence for this work. The authors also thank Dr. Quek Sung (Electrical Engineering at University of Manchester) for writing the Matlab program and IMEC for providing the waveguide coatings. Contents include material subject to Crown Copyright 2005 Dstl.

Received for review April 10, 2005. Accepted July 15, 2005.

AC050605J

(15) Woodside, S. M.; Bowen, B. D.; Piret, J. M. *Am. Inst. Chem. Eng. J.* **1997**, *43*, 1727–1736.